Environmental Toxicology and Chemistry—Volume 37, Number 9—pp. 2372–2379, 2018
Received: 24 January 2018 | Revised: 21 March 2018 | Accepted: 30 May 2018

Environmental Toxicology

Influence of Variable Ultraviolet Radiation and Oil Exposure Duration on Survival of Red Drum (*Sciaenops ocellatus*) Larvae

Kristin N. Bridges,[a,*] Michelle O. Krasnec,[b] Jason T. Magnuson,[a] Jeffrey M. Morris,[b] Michel L. Gielazyn,[c] J. Ruben Chavez,[d] and Aaron P. Roberts[a]

[a]Department of Biological Sciences & Advanced Environmental Research Institute, University of North Texas, Denton, Texas, USA
[b]Abt Associates, Boulder, Colorado, USA
[c]National Oceanic & Atmospheric Administration, Assessment & Restoration Division, St. Petersburg, Florida, USA
[d]Texas Parks and Wildlife Department, Coastal Fisheries Division, Corpus Christi, Texas, USA

Abstract: The toxicity of some polycyclic aromatic hydrocarbons (PAHs) increases with ultraviolet (UV) radiation. The intensity of UV radiation varies within aquatic ecosystems, potentially providing reprieves during which tissue repair may occur. Transient/short-term PAH exposure prior to UV exposure may initiate metabolism/clearance, potentially affecting outcomes. Larval *Sciaenops ocellatus* were exposed to oil and UV radiation, using either variable photoperiods or pre-UV oil exposure durations. Shorter PAH exposures exhibited greater toxicity, as did exposure to shorter photoperiods. *Environ Toxicol Chem* 2018;37:2372–2379. © 2018 SETAC

Keywords: Polycyclic aromatic hydrocarbon; Red drum; Oil spill; Deepwater Horizon; Photo-induced toxicity

INTRODUCTION

Polycyclic aromatic hydrocarbons (PAHs) are a class of contaminants composed of 2 or more fused carbon rings and are toxic constituents of crude oil (King 1988; MacFarland 1988; Cram et al. 2004). Characterized by high lipophilicity, persistence, and mutagenic and carcinogenic properties, these compounds are of particular concern following accidental oil and fuel releases (Weinstein 1996; Xue and Warshawsky 2005). Environmental factors, including ultraviolet (UV) radiation, influence the toxicity of PAHs. The presence of UV radiation can dramatically increase the toxicity of photodynamic PAHs, leading to adverse outcomes well below the threshold concentrations of other mechanisms of toxicity (Lyons et al. 2002; Diamond et al. 2006; Alloy et al. 2016) in a phenomenon called "photo-induced toxicity."

Models used to predict photo-induced toxicity report a reciprocal relationship where toxicity is a product of PAH and UV exposure (both intensity and duration; Oris and Giesy 1986). Adverse outcomes associated with this mechanism include increased mortality (Alloy et al. 2015; Damare et al. 2018), increased photo-avoidance behaviors (Oris and Giesy 1985), and decreased feeding behaviors (Hatch and Burton 1999). These effects have been well documented in a wide range of aquatic organisms, including fish (Alloy et al. 2016; Sweet et al. 2017), daphnia (Allred and Giesy 1985; Holst and Giesy 1989; Oris et al. 1990), bivalves (Lyons et al. 2002), marine diatoms (Wang et al. 2008), marine corals (Peachey and Crosby 1995), aquatic plants (Huang et al. 1997), and crabs (Alloy et al. 2015; Damare et al. 2018). Several of the aforementioned studies were conducted as a part of the Natural Resource Damage Assessment (NRDA) following the 2010 *Deepwater Horizon* oil spill in the Gulf of Mexico (Alloy et al. 2016, 2015; Morris et al. 2015; Sweet et al. 2017; Damare et al. 2018).

Red drum (*Sciaenops ocellatus*) is a commercially important fish species found in coastal areas along the Gulf of Mexico, which spawn between August and November, though this window can be shifted by several weeks depending on region (Davis 1990; Hatch and Burton 1999). Females release rapidly developing, positively buoyant eggs in relatively shallow open water. After hatch, larvae migrate to estuarine seagrass beds, where they remain until the juvenile stage (Davis 1990; Hatch and Burton 1999). Given its regional importance, life-history traits, and sensitivity to photo-induced toxicity, red drum is an important test species in the *Deepwater Horizon* NRDA (*Deepwater Horizon* Natural Resource Damage Assessment Trustees 2016; Alloy et al. 2017).

* Address correspondence to Kristin.bridges@unt.edu
Published online 1 June 2018 in Wiley Online Library (wileyonlinelibrary.com).
DOI: 10.1002/etc.4183

Exposure of biota to UV light in marine ecosystems varies because of a number of factors intrinsic to the water column (e.g., organic matter, photo-bleaching) and extrinsic factors (e.g., cloud cover, time of day; Hader et al. 1998; Weinstein and Diamond 2006). Tissue repair mechanisms may be differentially up-regulated when UV exposure is intermittent, potentially reducing toxicity because of sufficient repair during UV reprieves. Conversely, it may lead to a lag in initiating repair mechanisms (Weinstein and Diamond 2006). Therefore, it is important to understand how punctuated UV exposure influences outcomes for organisms co-exposed to PAHs, to improve models assessing risk (Weinstein and Diamond 2006).

Furthermore, metabolic processes may begin to degrade photodynamic PAHs over time, reducing body burdens and therefore decreasing the risk of adverse outcomes for the organism (Oris et al. 1990; Willis and Oris 2014). Metabolic clearance may occur prior to UV exposure or while organisms are in the presence of UV radiation. However, relatively little is known about the effects of transient PAH exposure prior to the introduction of UV radiation, a scenario that likely frequently occurs during accidental oil or fuel spills. Therefore, the goal of the present study was to evaluate how punctuated UV exposure periods and variable durations of PAH exposure (prior to UV exposure) affect survival of red drum larvae.

MATERIALS AND METHODS

Test organisms

Red drum larvae were obtained from Texas Parks and Wildlife Coastal Fisheries. All organisms were <48 h postfertilization and <24 hours post hatch at the start of testing.

Test solutions

The synthetic seawater used throughout testing was prepared with Milli-Q water and Instant Ocean® Sea Salts, with the following water quality parameters: salinity 33 ppt, pH 8.4, temperature 26 °C. Oil used for testing (hereafter referred to as "Slick A") was taken from the hold of barge CTC02404, collected from the *Deepwater Horizon* spill on 29 July 2010. Slick A oil was routinely used in photo-induced toxicity testing performed as part of the *Deepwater Horizon* NRDA (Alloy et al. 2016).

Stocks of a high-energy water accommodated fraction (HEWAF) were prepared with slick A oil using methods described in Alloy et al. (2016, 2015) at a loading rate of 1 g of oil in 1 L of seawater, which were further diluted in seawater to make test solutions. Samples of high and low dilutions were taken with each HEWAF preparation and shipped (at 4 °C) to ALS Environmental (Kelso, WA, USA) for analysis of PAHs. Extraction of PAHs was performed using US Environmental Protection Agency method 3541, prior to quantification of 50 selected PAHs (with the sum concentration of these analytes hereafter referred to as "$tPAH_{50}$"). Quantification was performed according to the methods outlined in Forth et al. (2017).

Toxicity tests

Glass crystalizing dishes containing 200 mL of test solutions were used as test chambers. All bioassays ended 24 h after the initial introduction of UV. Dishes were kept in a temperature-controlled chamber (26 °C) for the test duration, with no solution renewal. A standard toxicity test (no UV, 24 h) was performed in addition to photo-toxicity tests to examine the sensitivity of larval red drum to oil-only exposure. Indoor UV exposures were performed under light banks containing UV-A bulbs (described in Sweet et al. 2017), which were suspended above test chambers at a height yielding a UV-A intensity ($\lambda = 380$ nm) similar to that of solar radiation on a sunny day in the Gulf of Mexico, as measured by the Biospherical BIC radiometer (Sweet et al. 2017; Bridges et al. 2018). Incident UV_{380} was continuously measured throughout all tests (Table 1).

Test chambers were loaded with 10 larvae, with the exception of the 0-h PAH pre-exposure time test, which contained 20 larvae per dish. Dishes included in the PAH-only test (no UV) were assigned one of 8 PAH concentrations. Photo-toxicity tests were assigned to one of 2 categories: varying photoperiods (Figure 1A) or varying pre-UV PAH exposure durations (Figure 1B). In conjunction with the assigned photoperiod or PAH pre-exposure duration, each dish was also assigned one of 7 different PAH concentrations. Five replicates were used per treatment (defined as the combination of the specific photoperiod + designated

TABLE 1: Median lethal concentration (LC50) values and 95% confidence intervals (CIs) for all tests (24–28 h) with variations in integrated ultraviolet (UV; $\lambda = 380$ nm) dose and mean UV intensity included

Treatments					
Pre-UV PAH exposure (h)	UV photoperiod interval (h)	LC50 $tPAH_{50}$ (μg/L)[a]	95% CI	Total integrated UV dose ($mW \cdot s/cm^2$)	Mean UV intensity ±1 SD ($mW/cm^2/s$)
4	2	3.07	2.47–3.68	1457.8	0.051 ± 0.002
4	4	1.88	0.91–2.84	1680.9	0.059 ± 0.001
4	8	4.74	2.95–6.53	1680.9	0.059 ± 0.001
0	2	3.34	2.39–4.29	1463.5	0.051 ± 0.003
2	2	1.07	0.14–1.99	1457.8	0.051 ± 0.002
4	2	3.07	2.47–3.68	1457.8	0.051 ± 0.002

[a] See Figure 2 for a comparison of LC50 values calculated using the phototoxic dose.
$tPAH_{50}$ = total of 50 selected polycyclic aromatic hydrocarbons; SD = standard deviation.

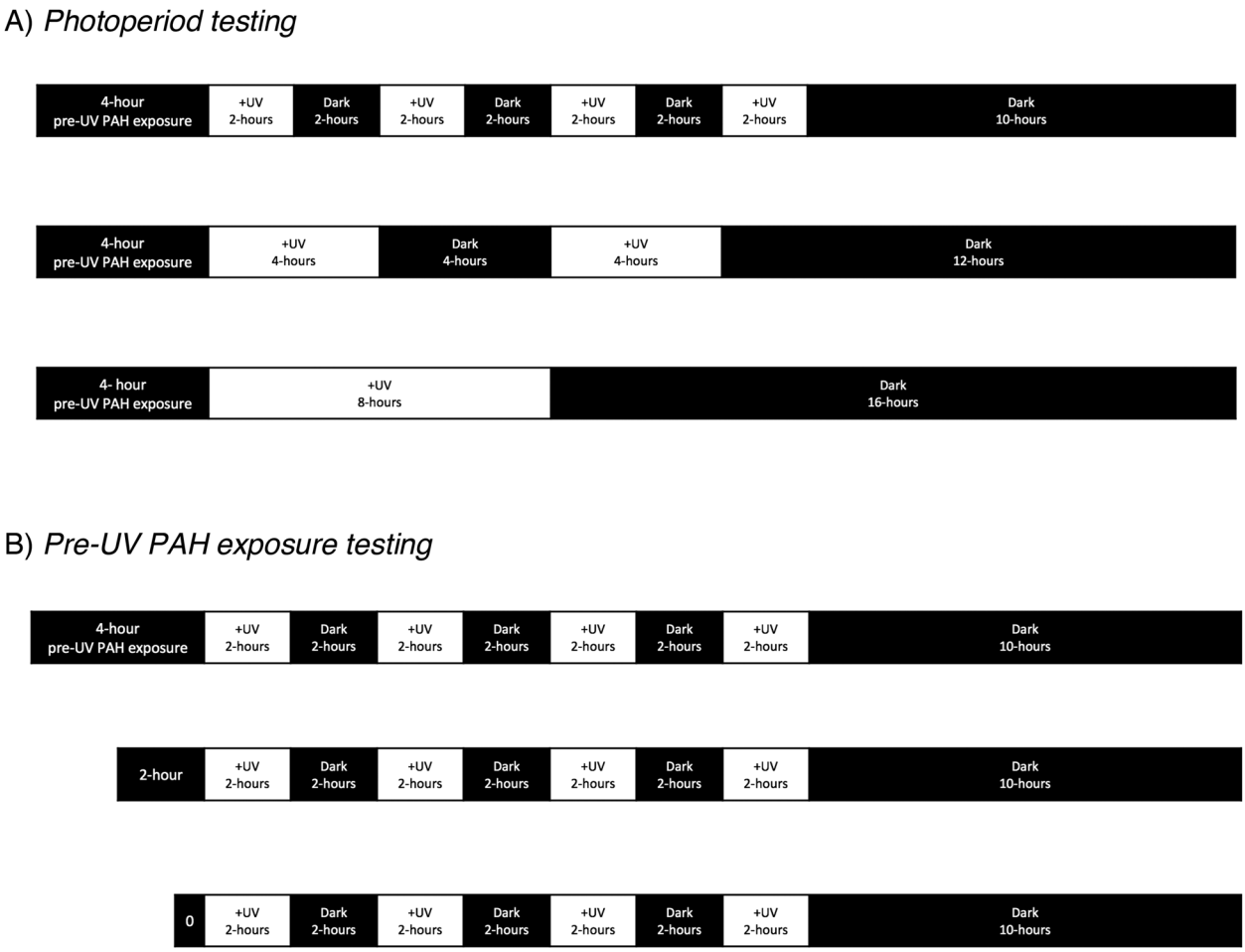

FIGURE 1: Diagrams displaying the experimental design of each ultraviolet (UV) exposure. (**A**) Exposure regimes during variable photoperiod testing. All treatments received a 4-h pre-UV polycyclic aromatic hydrocarbon (PAH) exposure duration, followed by a 2-, 4-, or 8-h UV exposure, which was repeated as necessary to reach a cumulative UV exposure time of 8 h. (**B**) Exposure regimes used during variable pre-UV PAH exposure testing. Following a 0-, 2-, or 4-h pre-UV PAH exposure, all treatments were exposed to UV in alternating 2-h photoperiods until a cumulative total of 8 h of UV was received.

PAH concentration or specific PAH pre-exposure duration + designated PAH concentration in photo-toxicity tests).

Test chambers assigned to the varying photoperiod category had a standardized 4-h pre-UV PAH exposure duration, followed by exposure to 8 h (cumulatively) of indoor UV-A radiation (Figure 1A) in the same exposure solution initially utilized (i.e., larvae were not moved to clean water following the pre-UV PAH exposure period). The UV exposure regimes were treatment-dependent and delivered in either 2-, 4-, or 8-h increments (photoperiods), with alternating UV-free recovery periods of the same duration (Figure 1A). The UV exposure cycle was repeated, as needed, until the cumulative UV exposure totaled 8 h for all treatments (range of integrated UV doses 1458–1681 $mW \cdot s/cm^2$; Table 1). Thereafter, the test chambers were kept in the dark until the conclusion of the test (i.e., 24 h after initiation of the first UV photoperiod). The total duration of these bioassays was 28 h.

Remaining test chambers were assigned to the PAH pre-exposure duration category. Treatments included 0-, 2-, or 4-h pre-UV PAH exposure durations (Figure 1B). The pre-UV PAH exposure and photoperiod durations for the 4-h treatment were identical to the parameters of the 2-h photoperiod treatment described previously; consequently, the data were shared between tests. Following the variable PAH pre-UV exposure period, all dishes were exposed to indoor UV-A radiation for a total of 8 h. The UV was delivered by repeating the following cycle: 2 h with UV, 2 h without UV, 4 times (cumulative UV exposure = 8 h, range of integrated UV doses 1458–1464; Figure 1B and Table 1). Thereafter, the test chambers were kept in the dark until the conclusion of the test (i.e., 24 h after initiation of the first UV photoperiod). The total duration of these bioassays ranged from 24 to 28 h.

Phototoxic units

Because of the number of tests conducted, it was necessary to perform tests over the course of several days. To account for slight variations in UV and PAH doses between tests, phototoxic doses were calculated to normalize the data, using the methods described in Alloy et al. (2016, 2015) and Sellin Jeffries et al. (2013). Briefly, molar concentrations of 14 known photodynamic PAHs (anthracene, benzo[*a*]anthracene, benzo[*e*]pyrene, benzo-[*g*,*h*,*i*]perylene, chrysene, fluoranthene, fluorene [C0, C1, C2],

phenanthrene [C0, C1, C2, C3], and pyrene) were calculated and multiplied by individual photodynamic activity relative to anthracene, to yield an anthracene equivalent molar concentration (in μM/L; Sellin Jeffries et al. 2013). The sum of the anthracene equivalent molar concentrations was then multiplied by the integrated UV_{380} irradiance (in $mW \cdot s/cm^2$) to produce the phototoxic dose (in $\mu M/L \cdot mW \cdot s/cm^2$).

Statistical analyses

To allow for a direct comparison of median lethal concentration (LC50) values between phototoxicity tests, it is necessary to generate dose–response curves using phototoxic dose as a predictor of mortality to account for variations in UV or PAH doses between tests (Alloy et al. 2016, 2015; Damare et al. 2018). However, we also report LC50 values as $tPAH_{50}$ (μg/L) to give context to the calculated phototoxic dose values. All LC50 values with 95% confidence intervals (CIs) were calculated from a logistic regression of the data, followed by an inverse prediction of 50% mortality using JMP software (Ver 13; SAS Institute). The same method was used to calculate the LC50 and 95% CI for the PAH-only (no UV) test, with $tPAH_{50}$ as the sole predictor of mortality. Within tests, treatments were determined to have significantly different LC50 values if there was no overlap in 95% CIs.

RESULTS

Red drum larvae were exposed to one of 7 slick A HEWAF dilutions, with measured PAH concentrations ranging from 0 to 14.87 μg/L $tPAH_{50}$. The total integrated UV (λ = 380 nm) doses for photoperiod tests ranged from 1458 to 1680 $mW \cdot s/cm^2$ and from 1458 to 1463 $mW \cdot s/cm^2$ for PAH pre-UV exposure tests (details in Table 1). Mean intensities ranged from 0.051 to 0.059 $mW/cm^2/s$ during photoperiod tests and were 0.051 $mW/cm^2/s$ during all PAH pre-exposures. Exposure concentrations used in the PAH-only test ranged from 0 to 925.2 μg/L $tPAH_{50}$. Survival of red drum larvae exposed to *Deepwater Horizon* slick A oil was adversely affected by PAH and UV exposure in a dose-dependent manner in all phototoxicity tests and by PAH concentration in the no-UV test.

The 28-h LC50 values (95% CI) for the 2-, 4-, and 8-h photoperiod tests were 3.07 (2.47–3.68), 1.88 (0.91–2.84), and 4.74 (2.95–6.53) μg/L $tPAH_{50}$, respectively (Table 1). Phototoxic dose LC50 values (95% CI) for these same tests (in order) were 2.23 (1.79–2.67), 1.57 (0.76–2.37), and 3.95 (2.46–5.46) $\mu M/L \cdot mW \cdot S/cm^2$ (Figure 2A). The LC50 values for the 2-h photoperiod test were not significantly different from those of the 4-h photoperiod test (as seen by overlapping 95% CIs), though the 2-h photoperiods appeared to be slightly less toxic. However, both the phototoxic and $tPAH_{50}$ LC50 values from the 4-h photoperiod test were significantly lower than those for the 8-h photoperiod treatment, with no overlap in the 95% CIs between treatments. It should be noted that there is a slight overlap in the 95% confidence intervals between the 2 and 8-h photoperiod tests because of the wide CI from the 8-h test.

The 24- to 28-h LC50 values (95% CI) for the 0-, 2-, and 4-h PAH pre-UV exposure duration tests were 3.34 (2.39–4.29), 1.07 (0.14–1.99), and 3.07 (2.47–3.68) μg/L $tPAH_{50}$ (Table 1), with phototoxic dose LC50 values (95% CI) of 2.55 (1.83–3.27), 0.78 (0.10–1.45), and 2.23 (1.79–2.67) $\mu M/L \cdot mW \cdot S/cm^2$, respectively. The 2-h PAH pre-UV exposure test resulted in significantly greater toxicity relative to the treatment receiving no PAH pre-exposure (0 h) and the 4-h PAH pre-UV exposure.

The 24-h LC50 (95% CI) for the no-UV toxicity test was 79.94 (52.94–106.94) μg/L $tPAH_{50}$. In comparison with the range of LC50 values (μg/L $tPAH_{50}$) derived from the UV photo-toxicity tests, the addition of UV radiation resulted in a 15- to 75-fold increase in toxicity.

DISCUSSION

The toxicity of *Deepwater Horizon* oil to larval red drum increased by as much as 75 times with the addition of UV exposure in the present study (e.g., 79.94 vs 1.07 μg/L $tPAH_{50}$ in the no-UV and 2-h pre-UV exposure tests, respectively). This amplification of toxicity in the presence of UV radiation highlights the importance of considering UV photo-toxicity in risk and injury assessments involving oil spills. Concentrations

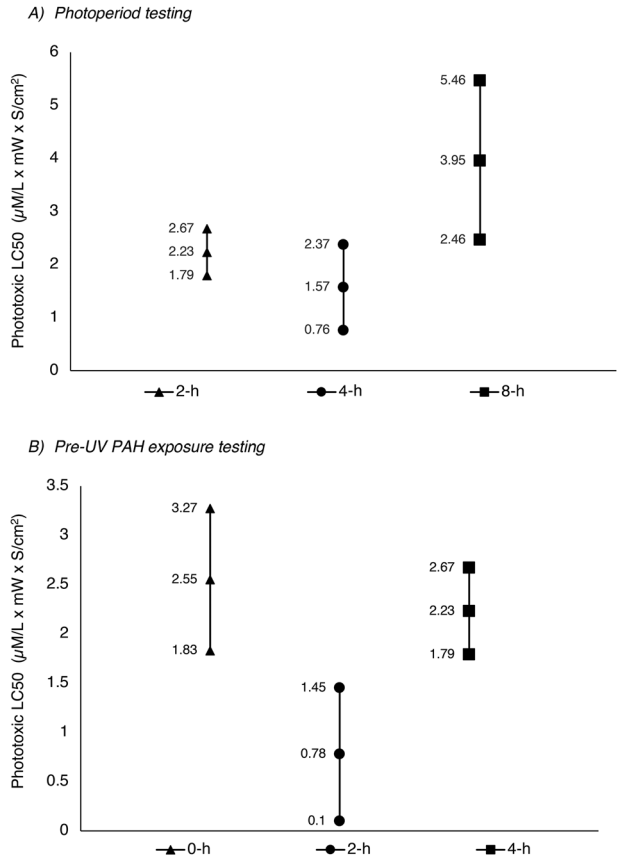

FIGURE 2: Phototoxic median lethal concentrations (LC50s) calculated by test type. (**A**) The 28-h LC50 values surrounded by 95% confidence intervals (CIs) for treatments receiving a 4-h pre-ultraviolet (UV) polycyclic aromatic hydrocarbon (PAH) exposure and one of the 2-, 4-, or 8-h photoperiod UV exposure regiments. (**B**) The 24- to 28-h LC50 values surrounded by 95 CIs for treatments receiving one of the 0-, 2-, or 4-h pre-UV PAH exposures followed by a cumulative total of 8 h of UV exposure, delivered using the 2-h photoperiod cycles.

recorded in the area impacted by the *Deepwater Horizon* spill ranged from 0 to 84.8 μg/L $tPAH_{50}$. Concentrations used in the present study fall within the lower range of recorded concentrations during the spill (*Deepwater Horizon* Natural Resource Damage Assessment Trustees 2016; Forth et al. 2017). Furthermore, postspill water sample data collected from several sites in the Gulf of Mexico indicate that complete attenuation of oil took nearly a year in most instances, with one site exhibiting increased concentrations several years later (Allan et al. 2012). This persistence, coupled with the environmentally relevant $tPAH_{50}$ concentrations and UV doses (Bridges et al. 2018) used in the present study, are likely representative of exposure scenarios in the field following the spill. Furthermore, the LC50 values reported in the present study are within the range reported in other studies (Table 2) investigating photo-induced toxicity of *Deepwater Horizon* oil to early–life stage organisms (Alloy et al. 2016, 2015; Finch et al. 2016; Sweet et al. 2017; Damare et al. 2018). Therefore, the present LC50 values are likely to be of environmental relevance and represent possible outcomes for early–life stage organisms exposed to solar radiation in oiled habitats.

The results of variable photoperiod tests suggest that shorter intervals of UV exposure over an 8-h period increase oil toxicity compared to an uninterrupted 8-h UV exposure, even though cumulative UV exposure hours and phototoxic doses are equivalent (Figure 2A). Ultimately, outcomes for organisms co-exposed to UV and PAHs are determined by the net tissue damage sustained during exposure, minus repair that occurs in the absence of a stressor(s), (Oris and Giesy 1986). Despite receiving equal phototoxic doses, the 2- and 4-h photoperiod treatments concluded their final UV exposure 14 and 12 h (respectively) after the initial introduction of UV, while UV exposure ceased after 8 h in the continuous UV treatment. The data suggest that the total number of hours between the first and last UV exposures (including periods of reprieve from UV), rather than simply the number of hours that UV is actually present, and the pattern in which the total integrated UV dose is delivered are factors in determining the photo-induced toxicity of PAHs to larval red drum.

Studies examining the role of biological recovery in photo-induced toxicity in fish are scarce, and to our knowledge, ours is the first to report the effects of photo-period durations that last less than 6 h on survival. However, a few photo-induced toxicity studies using single PAH exposures (rather than the complex mixture of PAHs present in oil) and photo-period durations ranging from 6 to 24 h have been conducted. Weinstein (2002) reported an absence of repair in glochidia of the freshwater mussel *Utterbackia imbecillis* co-exposed to fluoranthene and UV, using photoperiods ranging from 8 to 24 h. Oris and Giesy (1986) found that LC50 was significantly affected by photoperiod length (6–24 h) in juvenile bluegill sunfish (*Lepomis macrochirus*) co-exposed to anthracene, providing evidence for repair. It is worth noting that significant acute mortality still occurred in that study, attributable to cumulative tissue damage after several cycles of UV exposure (Oris and Giesy 1986). The results of these studies combined with the present results indicate that recovery capacity varies according to species, life stage, and photoperiod duration.

The primary mode of action associated with photo-induced toxicity is cell membrane disruption by reactive oxygen species (ROS; Weinstein et al. 1997; Choi and Oris 2000). Repair of oxidized lipids is an energetically costly and rate-limited process, relying on a number of enzymes, antioxidants, and available fatty acids (Van Kuijk et al. 1987; Gregus and Klaassen 2001). Red drum larvae used in the present study were less than 3 d posthatch and were therefore still using their attached, lipid-rich

TABLE 2: Median lethal concentration (LC50) values reported in the literature from various photo-induced toxicity tests using *Deepwater Horizon* oil and early–life stage marine organisms[a]

Organism	LC50 (μg/L $tPAH_{50}$)	PAH exposure (h)	Photoperiod duration (h)	Phototoxic LC50 ($\mu M/L \cdot mW \cdot S/cm^2$)	Oil type	UV type
Blue crab zoae (Alloy et al. 2015)	N/A	17	7 (× 2 exposures)	9.5	Slick A HEWAF	Solar
Fiddler crab zoae (Damare et al. 2018)	5.12	17	7 (× 2 exposures)	2.96	Slick A HEWAF	Solar
Seatrout larvae (Alloy et al. 2017)	0.83	8	6	0.52	Slick A HEWAF	Solar
Red drum larvae (Alloy et al. 2017)	3.42	8	6	1.41	Slick A HEWAF	Solar
Red drum larvae (present study)	1.88	4	4	1.57	Slick A HEWAF	Indoor
Mahi-mahi embryos (<24 hpf; Alloy et al. 2016)	N/A	17	7 (× 2 exposures)	6.77[b]	Slick A HEWAF	Solar
Mahi-mahi embryos (28 hpf; Sweet et al. 2017)	10[b]	28	8	5.4[b]	Oil from surface HEWAF	Indoor
Mysid shrimp (72 h; Finch et al. 2017)	3.19	16-19	1 diurnal period	N/A	Slick A LEWAF	Solar
Mysid shrimp	0.82	15	6	N/A	Slick A HEWAF	Solar
Inland silverside (7 dph; also Finch et al. 2017)	6.86	16–19	1 diurnal period	N/A	Slick A LEWAF	Solar
Eastern oyster larvae (2–4 hpf; Finch et al. 2016)	5.03	0	6	N/A	Slick A LEWAF	Indoor

[a] Organisms are <24 h old unless otherwise specified.
[b] Values reported as median effective concentration (rather than LC50) for hatch success.
dph = days post hatch; HEWAF = high-energy water accommodated fraction; hpf = hours postfertilization; LEWAF = low-energy water accommodated fraction; N/A = not analyzed; $tPAH_{50}$ = total of 50 selected polycyclic aromatic hydrocarbons; UV = ultraviolet.

yolk sacs as their energy source (Davis 1990). Consequently, limited resources (which are also subject to damage by ROS) are available at this life stage to repair peroxidized lipids (Vetter et al. 1983; Tocher et al. 1985). Lipid peroxidation is self-propagating because of the generation of reactive intermediates (Niki et al. 2005). Given that the stress experienced by the larvae appeared to be dependent on the length of time between the first and last UV exposures, it is possible that the aforementioned factors led to continued tissue damage and energy depletion during dark periods, amplified at the commencement of each photoperiod.

Increased ventilation rates, which are directly related to metabolic rate, have also been observed in juvenile bluegill sunfish (*L. macrochirus*) co-exposed to anthracene and UV radiation (McCloskey and Oris 1991; Millidine et al. 2008). Changes in ventilation in more mature life stages of fish are attributed to lipid peroxidation of membrane surfaces at the gills, which increases in a time-dependent manner (Weinstein et al. 1997). Larval red drum lack respiratory pigments in their blood and respire through cutaneous diffusion, increasing the risk of altered respiration from photo-induced toxicity as PAH accumulates in lipid-rich, transparent cells on the body surface (Torres et al. 1996; Willis and Oris 2014). As previously discussed, the total stress experienced by larvae appeared to be dependent on the length of time between the first and last UV exposures (Figure 1B), rather than the presence of rest periods. Therefore, it appears likely that a combination of these factors contributed to increased energy depletion in larvae from the 2 and 4-h treatments, resulting in higher mortality.

It should be noted that our chemistry analysis was performed on diluted HEWAF samples taken at the beginning of the test, rather than at the conclusion of the study. Test solutions were not renewed, and therefore photo-degradation of PAHs in test solutions may have occurred over the course of the test. Loss of slick A HEWAF has been shown to occur most rapidly within the first 24 h; however, Forth et al. (2017) concluded that PAH loss impacts the chemistry of high-concentration HEWAFs to a much greater extent than the very low concentrations used in the present study. We would also expect the 8-h treatment to be the most toxic if PAH loss in the early hours of the exposure alone explained the difference in toxicity between treatments. Thus, it is likely that biological factors are driving the differential toxicity between photoperiods. It is worth noting that, regardless of treatment type, PAH concentrations used in the present study were measured at the beginning of the exposure. Therefore, the LC50s we report may underestimate toxicity because they do not account for PAH loss.

The duration that organisms were exposed to oil prior to UV exposure affected toxicity. Greater toxicity was observed in the 2-h pre-UV PAH exposure test relative to both the 4-h test as well as the test with no pre-UV exposure to PAH (Figure 2B). Differences in toxicity between pre-UV PAH exposure durations are likely the result of variable internal PAH doses (body burdens), which are determined by the combined effects of uptake and elimination (Arnot and Gobas 2006; Willis and Oris 2014). The treatment that received no pre-UV PAH exposure showed significantly reduced toxicity relative to the 2-h treatment, despite receiving an identical UV dose. Because photo-toxicity is both PAH- and UV-dependent, these results may indicate that the PAH body burden was low enough prior to UV exposure to result in reduced toxicity.

Similarly, the LC50 was significantly higher in the 4-h pre-UV PAH exposure treatment relative to the 2-h treatment, despite identical UV exposures, suggesting lower body burden of PAHs in the 4-h treatment. There may be a threshold duration of low-level PAH exposure (prior to the introduction of UV) at which metabolic processes in larval red drum exceed uptake rates, resulting in lower body burdens and better survival. Results of several studies indicate that metabolism of PAHs in teleosts begins a very short time after initial exposure, with maximum concentrations of benzo[*a*]pyrene metabolites detected in rainbow trout (*Salmo gairdneri*) gills 25 to 40 min after exposure (Andersson and Pärt 1989; Baussant et al. 2001; Hornung et al. 2007; Mathew et al. 2008; Willis and Oris 2014). Though there are species- and life stage–dependent variations in metabolic capacity, biotransformation of PAHs has even been confirmed in embryonic fish (Baussant et al. 2001; Hornung et al. 2007; Mathew et al. 2008; Sorensen et al. 2017). The greatest toxicity in the present study was observed in the treatment exposed to PAHs for 2 h prior to introduction of UV, which may be explained by higher body burdens (relative to other treatments) at the time UV is introduced. It is plausible that the 2-h PAH exposure duration is sufficient to achieve elevated PAH body burdens (at the low PAH concentrations used in the present study), whereas biotransformative processes require slightly longer to up-regulate.

As previously mentioned, the $tPAH_{50}$ values reported in the present study are based on the those measured in samples of testing solutions that were collected immediately after preparation. We did not renew solutions during testing, and some amount of PAH loss from the testing chambers can be expected to occur over time (Forth et al. 2017). Therefore, it is plausible that the toxicity values reported for the present study underestimate hazard because we did not calculate time-integrated PAH doses (Alloy et al. 2016), which would have resulted in lower LC50 values.

Alloy et al. (2016) reported a phototoxic LC50 of 1.41 μM/L · mW · S/cm^2 (CI 1.17–1.65 μM/L · mW · s/cm^2) in red drum larvae of comparable age after an 8-h pre-UV PAH exposure using similar concentrations of slick A HEWAF (range 0–11.76 μg/L $tPAH_{50}$), followed by a 6-h solar exposure (total integrated UV dose 705.79 mW · s/cm^2, intensity 0.038 ± 0.021). An 8-h pre-UV PAH exposure/6-h UV exposure scenario was not used in the present study because the longest pre-UV PAH exposure duration was 4 h. Therefore, a direct comparison is not possible. However, a comparable treatment from the present study (4-h pre-UV PAH exposure/4-h photoperiod) yielded a phototoxic LC50 of 1.57 μM/L · mW · S/cm^2, which is within the 95% CI of the LC50 reported by Alloy et al. (2016). Interestingly, the 8-h pre-UV PAH exposure duration used by Alloy et al. did not appear to significantly increase toxicity to red drum larvae relative to the results of the 4-h pre-UV PAH exposure treatment from the present study. This supports the explanation that pre-UV PAH exposure durations which persist long enough to allow the organism to initiate a metabolic response to PAH presence

may decrease toxicity by allowing a window of PAH clearance prior to introduction of UV.

In natural systems, UV exposure constantly fluctuates, and variable PAH exposure prior to the introduction of UV can be expected to occur at spill sites (Weinstein and Diamond 2006). Therefore, it is important to understand how alterations in these parameters impact the predictive capability of the reciprocity model, which states that at equal phototoxic doses the phototoxic effect will be equal. All tests exhibited dose-dependent mortality by UV and PAH exposure in the present study, indicating that the current model of photo-induced toxicity provides an important framework for predicting phototoxic effects on biota. However, variations in both UV photoperiod and pre-UV PAH exposure durations yielded significant variations in LC50 values at equal phototoxic doses. This variable sensitivity indicates a potential for the reciprocity model to underpredict or overpredict PAH photo-induced toxicity under certain environmental conditions. However, it should be noted that the differences in LC50 are within just a few μg/L. Given the complexity of conditions in the natural environment, it is likely that these differences in LC50 would fall within the natural variation in PAH concentrations during an oil spill event. Thus, these findings support the simple extrapolation of laboratory-based photo-induced toxicity tests to the field even if they may vary slightly in PAH exposure time/UV exposure duration. More research is needed to determine how other environmental factors may affect the predictive capabilities of the reciprocity model.

Chronic studies examining the latent effects of sublethal PAH photo-induced toxicity on *Daphnia magna* have demonstrated significant effects on reproduction (Holst and Giesy 1989), followed by significant latent mortality after the removal of UV (Gnau 2017). It is possible that these effects are attributable to tissue damage sustained during the initial co-exposure period, the continued presence of photo-oxidized PAH compounds, or a combination of these factors (King et al. 2014; Roberts et al. 2017). Regardless, these endpoints have potential implications for recruitment of young to the population, with potential population/community structure impacts. The findings of those studies, together with the present results, have important implications for assessing risk and injury to aquatic organisms exposed to PAHs and UV light over short durations in the environment.

Acknowledgment—The authors thank B. Soulen and E. Barnes (University of North Texas) and I. Lipton, A. McFadden, and C. Lay (Abt Associates) for their assistance. The present study was conducted within *the Deepwater Horizon* NRDA investigation, which was cooperatively conducted by the National Oceanic and Atmospheric Administration (NOAA) and other federal and state trustees. Funds for the present study were provided as part of the NRDA for the *Deepwater Horizon* oil spill (NOAA contract AB133C-11-CQ-0051).

Disclaimer—The scientific results and conclusions of the present publication are those of the authors and do not necessarily represent the official policy or opinion of National Oceanic and Atmospheric Administration or any other natural resource trustee for the BP/*Deepwater Horizon* NRDA. Any use of trade, firm, or product names is for descriptive purposes only and does not imply endorsement by the US government.

Data Availability—Data are available on request from Aaron P. Roberts (aproberts@unt.edu).

REFERENCES

Allan SE, Smith BW, Anderson KA. 2012. Impact of the *Deepwater Horizon* oil spill on bioavailable polycyclic aromatic hydrocarbons in Gulf of Mexico coastal waters. *Environ Sci Technol* 46:2033–2039.

Alloy M, Baxter D, Stieglitz J, Mager E, Hoenig R, Benetti D, Grosell M, Oris J, Roberts A. 2016. Ultraviolet radiation enhances the toxicity of *Deepwater Horizon* Oil to mahi-mahi (*Coryphaena hippurus*) embryos. *Environ Sci Technol* 50:2011–2017.

Alloy M, Garner TR, Bridges K, Mansfield C, Carney M, Forth H, Krasnec M, Lay C, Takeshita R, Morris J, Bonnot S, Oris J, Roberts A. 2017. Co-exposure to sunlight enhances the toxicity of naturally weathered *Deepwater Horizon* oil to early lifestage red drum (*Sciaenops ocellatus*) and speckled seatrout (*Cynoscion nebulosus*). *Environ Toxicol Chem* 36:780–785.

Alloy MM, Boube I, Griffitt RJ, Oris JT, Roberts AP. 2015. Photo-induced toxicity of *Deepwater Horizon* slick oil to blue crab (*Callinectes sapidus*) larvae. *Environ Toxicol Chem* 34:2061–2066.

Allred PM, Giesy JP. 1985. Solar radiation–induced toxicity of anthracene to *Daphnia pulex*. *Environ Toxicol Chem* 4:219–226.

Andersson T, Pärt P. 1989. Benzo[*a*]pyrene metabolism in isolated perfused rainbow trout gills. *Mar Environ Res* 28:3–7.

Arnot JA, Gobas FAPC. 2006. A review of bioconcentration factor (BCF) and bioaccumulation factor (BAF) assessments for organic chemicals in aquatic organisms. *Environ Rev* 14:257–297.

Baussant T, Sanni S, Skadsheim A, Jonsson G, Borseth JF, Gaudebert B. 2001. Bioaccumulation of polycyclic aromatic compounds: 2. Modeling, bioaccumulation in marine organisms chronically exposed to dispersed oil. *Environ Toxicol Chem* 20:1185–1195.

Bridges K, Lay C, Alloy M, Gielazyn M, Morris J, Forth H, Takeshita R, Travers C, Oris J, Roberts A. 2018. Estimating incident ultraviolet (UV) radiation exposure in the northern Gulf of Mexico during the *Deepwater Horizon* oil spill. *Environ Toxicol Chem* 37:1679–1687.

Choi J, Oris JT. 2000. Evidence of oxidative stress in bluegill sunfish (*Lepomis macrochirus*) liver microsomes simultaneously exposed to solar ultraviolet radiation and anthracene. *Environ Toxicol Chem* 19:1795–1799.

Cram S, Siebe C, Ortź-Salinas R, Herre A. 2004. Mobility and persistence of petroleum hydrocarbons in peat soils of southeastern Mexico. *Soil Sediment Contam* 13:341–360.

Damare LM, Bridges KN, Alloy MM, Curran TE, Soulen BK, Forth HP, Lay CR, Morris JM, Stoeckel JA, Roberts AP. 2018. Photo-induced toxicity in early life stage fiddler crab (*Uca longisignalis*) following exposure to *Deepwater Horizon* oil. *Ecotoxicology* 27:440–447.

Davis JT. 1990. Red drum: Biology and life history. SRAC Publication 320. Southern Regional Aquaculture Center, Stoneville, MS, USA.

Deepwater Horizon Natural Resource Damage Assessment Trustees. 2016. Final programmatic damage assessment and restoration plan and final programmatic environmental impact statement. Wahsington DC, USA. [cited 2017 July 26]. Available from: http://www.gulfspillrestoration.noaa.gov/restoration-planning/gulf-plan

Diamond SA, Mount DR, Mattson VR, Heinis LJ. 2006. Photoactivated polycyclic aromatic hydrocarbon toxicity in medaka (*Oryzias latipes*) embryos: Relevance to environmental risk in contaminated sites. *Environ Toxicol Chem* 25:3015–3023.

Finch BE, Stefansson ES, Langdon CJ, Pargee SM, Blunt SM, Gage SJ, Stubblefield WA. 2016. Photo-enhanced toxicity of two weathered Macondo crude oils to early life stages of the eastern oyster (*Crassostrea virginica*). *Mar Pollut Bull* 113(1–2):316–323.

Finch BE, Marzooghi S, Di Toro DM, Stubblefield WA. 2017. Phototoxic potential of undispersed and dispersed fresh and weathered Macondo crude oils to Gulf of Mexico marine organisms. *Environ Toxicol Chem* 36:2640–2650.

Forth HP, Mitchelmore CL, Morris JM, Lay CR, Lipton J. 2017. Characterization of dissolved and particulate phases of water accommodated fractions

used to conduct aquatic toxicity testing in support of the *Deepwater Horizon* natural resource damage assessment. *Environ Toxicol Chem* 36:1460–1472.

Gnau J. 2017. Evaluating the role of UV exposure and recovery regimes in PAH photo-induced toxicity to *Daphnia magna*. Master's thesis. University of North Texas, Denton, TX, USA.

Gregus Z, Klaassen CD. 2001. Mechanisms of toxicity. In: Klaassen CD, ed, *Casarett and Doull's Toxicology: The Basic Science of Poisons*, 6th ed. McGraw-Hill, New York, NY, USA, pp 35–82.

Hader DP, Kumar HD, Smith RC, Worrest RC. 1998. Effects on aquatic ecosystems. *J Photochem Photobiol B* 46(1–3):53–68.

Hatch AC, Burton GA. 1999. Photo-induced toxicity of PAHs to *Hyalella azteca* and *Chironomus tentans*: Effects of mixtures and behavior. *Environ Pollut* 106:157–167.

Holst LL, Giesy JP. 1989. Chronic effects of the photoenhanced toxicity of anthracene on *Daphnia magna* reproduction. *Environ Toxicol Chem* 8:933–942.

Hornung MW, Cook PM, Fitzsimmons PN, Kuehl DW, Nichols JW. 2007. Tissue distribution and metabolism of benzo[*a*]pyrene in embryonic and larval medaka (*Oryzias latipes*). *Toxicol Sci* 100:393–405.

Huang XD, McConkey BJ, Babu TS, Greenberg BM. 1997. Mechanisms of photoinduced toxicity of photomodified anthracene to plants: Inhibition of photosynthesis in the aquatic higher plant *Lemna gibba* (duckweed). *Environ Toxicol Chem* 16:1707–1715.

King RW. 1988. Petroleum: Its composition, analysis and processing. *Occup Med* 3:409–430.

King SM, Leaf PA, Olson AC, Ray PZ, Tarr MA. 2014. Photolytic and photocatalytic degradation of surface oil from the *Deepwater Horizon* spill. *Chemosphere* 95:415–422.

Lyons BP, Pascoe CK, McFadzen IR. 2002. Phototoxicity of pyrene and benzo[*a*]pyrene to embryo-larval stages of the Pacific oyster *Crassostrea gigas*. *Mar Environ Res* 54(3–5):627–631.

MacFarland HN. 1988. Toxicology of petroleum hydrocarbons. *Occup Med* 3:445–454.

Mathew R, McGrath JA, Di Toro DM. 2008. Modeling polycyclic aromatic hydrocarbon bioaccumulation and metabolism in time-variable early life-stage exposures. *Environ Toxicol Chem* 27:1515–1525.

McCloskey JT, Oris JT. 1991. Effect of water temperature and dissolved oxygen concentration on the photo-induced toxicity of anthracene to juvenile bluegill sunfish (*Lepomis macrochirus*). *Aquat Toxicol* 21:145–156.

Millidine KJ, Metcalfe NB, Armstrong JD. 2008. The use of ventilation frequency as an accurate indicator of metabolic rate in juvenile Atlantic salmon (*Salmo salar*). *Can J Fish Aquat Sci* 65:2081–2087.

Morris J, Krasnec MO, Carney M, Forth H, Lay C, Lipton I, McFadden A, Takeshita R, Cacela D, Holmes JV, Lipton J; Abt Associates. 2015. *Deepwater Horizon* Oil Spill Natural Resource Damage Assessment Comprehensive Toxicity Testing Program: Overview, methods, and results. Technical Report. National Oceanic and Atmospheric Administration, Seattle, WA, USA. [cited 2017 July 26]. Available from: https://www.fws.gov/doiddata/dwh-ar-documents/952/DWH-AR0293761.pdf

Niki E, Yoshida Y, Saito Y, Noguchi N. 2005. Lipid peroxidation: Mechanisms, inhibition and biological effects. *Biochem Biophys Res Commun* 338:668–676.

Oris JT, Giesy JP. 1986. Photoinduced toxicity of anthracene to juvenile bluegill sunfish (*Lepomis macrochirus* Rafinesque): Photoperiod effects and predictive hazard evaluation. *Environ Toxicol Chem* 5:761–768.

Oris JT, Giesy JP. 1985. The photoenhanced toxicity of anthracene to juvenile sunfish (*Lepomis* spp.). *Aquat Toxicol* 6:133–146.

Oris JT, Hall AT, Tylka JD. 1990. Humic acids reduce the photo-induced toxicity of anthracene to fish and daphnia. *Environ Toxicol Chem* 9:575–583.

Peachey RL, Crosby DG. 1995. Phototoxicity in a coral reef flat community. In Gulko D, Jokiel PL, eds, *Ultraviolet Radiation and Coral Reefs*. Hawaii Institute of Marine Biology Technical Report 41. University of Hawaii Sea Grant Publication UNIHI-SEAGRANT-CR-95-03. Kaneohe, HI, USA, pp 193–200.

Roberts AP, Alloy MM, Oris JT. 2017. Review of the photo-induced toxicity of environmental contaminants. *Comp Biochem Physiol C Toxicol Pharmacol* 191:160–167.

Sellin Jeffries MK, Claytor C, Stubblefield W, Pearson WH, Oris JT. 2013. Quantitative risk model for polycyclic aromatic hydrocarbon photoinduced toxicity in Pacific herring following the *Exxon Valdez* oil spill. *Environ Sci Technol* 47:5450–5458.

Sorensen L, Sorhus E, Nordtug T, Incardone JP, Linbo TL, Giovanetti L, Karlsen O, Meier S. 2017. Oil droplet fouling and differential toxicokinetics of polycyclic aromatic hydrocarbons in embryos of Atlantic haddock and cod. *PLoS One* 12:26.

Sweet LE, Magnuson J, Garner TR, Alloy MM, Stieglitz JD, Benetti D, Grosell M, Roberts AP. 2017. Exposure to ultraviolet radiation late in development increases the toxicity of oil to mahi-mahi (*Coryphaena hippurus*) embryos. *Environ Toxicol Chem* 36:1592–1598.

Tocher DR, Frasner AJ, Sargent JR, Gamble C. 1985. Lipid class composition during embryonic and early larval development in Atlantic herring (*Clupea harangues*, L.). *Lipids* 20:84–89.

Torres JJ, Brightman RI, Donnelly J, Harvey J. 1996. Energetics of larval red drum, *Sciaenops ocellatus*. 1. Oxygen consumption, specific dynamic action, and nitrogen excretion. *Fish Bull (Wash DC)* 94:756–765.

Van Kuijk F, Sevanian A, Handelman G, Dratz E. 1987. A new role for phospholipase A2: Protection of membranes from lipid peroxidation damage. *Trends Biochem Sci* 12:31–34.

Vetter RD, Hodson RE, Arnold C. 1983. Energy metabolism in a rapidly developing marine fish egg, the red drum (*Sciaenops ocellata*). *Can J Fish Aquat Sci* 40:627–634.

Wang LP, Zheng BH, Meng W. 2008. Photo-induced toxicity of four polycyclic aromatic hydrocarbons, singly and in combination, to the marine diatom *Phaeodactylum tricornutum*. *Ecotoxicol Environ Saf* 71:465–472.

Weinstein JE. 1996. Anthropogenic impacts on salt marshes—A review. In Vernberg FJ, Vernberg WB, Siewicki T, eds, *Sustainable Development in the Southeastern Coastal Zone*. Belle W. Baruch Library in Marine Science 20. University of South Carolina, Columbia, SC, USA, pp 135–170.

Weinstein JE. 2002. Photoperiod effects on the UV-induced toxicity of fluoranthene to freshwater mussel glochidia: Absence of repair during dark periods. *Aquat Toxicol* 59(3–4):153–161.

Weinstein JE, Diamond SA. 2006. Relating daily solar ultraviolet radiation dose in salt marsh–associated estuarine systems to laboratory assessments of photoactivated polycyclic aromatic hydrocarbon toxicity. *Environ Toxicol Chem* 25:2860–2868.

Weinstein JE, Oris JT, Taylor DH. 1997. An ultrastructural examination of the mode of UV-induced toxic action of fluoranthene in the fathead minnow, *Pimephales promelas*. *Aquat Toxicol* 39:1–22.

Willis AM, Oris JT. 2014. Acute photo-induced toxicity and toxicokinetics of single compounds and mixtures of polycyclic aromatic hydrocarbons in zebrafish. *Environ Toxicol Chem* 33:2028–2037.

Xue W, Warshawsky D. 2005. Metabolic activation of polycyclic and heterocyclic aromatic hydrocarbons and DNA damage: A review. *Toxicol Appl Pharmacol* 206:73–93.

